Desalination and Water Treatment
www.deswater.com

doi: 10.5004/dwt.2021.27730

237 (2021) 202–213
October

Removal of uranium(VI) and thorium(IV) from aqueous solution by *Hedera helix* leaves: kinetics and thermodynamic studies

Faten M. Abu Orabi[a,b,*], Fawwaz I. Khalili[a], Latifa S. Ismail[a]

[a]*Chemistry Department, The University of Jordan, Amman 11942, Jordan, Tel. +962 6535000; emails: fatenaladwan_i@yahoo.com (F.M. Abu Orabi), fkhalili@ju.edu.jo (F.I. Khalili), latifa.saeed@yahoo.com (L.S. Ismail)*
[b]*Department of Chemistry, Faculty of Arts and Science, Applied Science Private University, Amman 11931, Jordan*

Received 15 February 2021; Accepted 4 August 2021

ABSTRACT

In this research, *Hedera helix* leaves were evaluated for biosorption of uranium(VI) and thorium(IV) ions from aqueous solution. *H. helix* leaves were characterized by Fourier-transform infrared spectroscopy, X-ray diffraction, thermal gravimetric analysis and scanning electron microscope. Biosorption of uranium(VI) and thorium(IV) ions using a batch technique by *H. helix* leaves was evaluated as a function of metal concentration, adsorbent dose, contact time, pH and temperature. The results of biosorption kinetic show that biosorption of U(VI) and Th(IV) by *H. helix* leaves was well described by the pseudo-second-order kinetic model. Negative values of Gibbs free energy $\Delta G°$ indicate the spontaneity of the biosorption process on *H. helix* leaves, while the positive values of enthalpy $\Delta H°$ indicate the endothermic process. The biosorption isotherm was better fitted by Langmuir isotherm, with a maximum biosorption capacity of 3.86 and 5.16 mg/g for U(VI) and Th(IV) respectively. Desorption studies show that 75% of U(VI) was recovered using 0.1 M HNO_3 after four cycles, while 87.7% of Th(IV) was recovered using 1.0 M HNO_3 after four cycles.

Keywords: Biosorption; Uranium(VI); Thorium(IV); *Hedera helix* leaves; Kinetics; Thermodynamics

1. Introduction

Uranium and thorium are the most natural abundant actinide elements that are of special interest in the modern industry such as battery and pigment manufacturing, defense operations (nuclear weapon) and as a fuel in a nuclear reactor for electrical power production [1,2]. Where nuclear fission reactions release huge amounts of energy and huge amounts of wastes containing these radionuclides that accumulated in the environment and water sources [3,4]. Also, they accumulate through the natural weathering of ore minerals and rocks [5]. So, separation and pre-concentration of these radionuclide elements from contaminated wastes before dispose in the environment will minimize pollution and shall increase the possibilities for metal recovery which is important economically [6].

The most popular methods used for metal pollutants removal from wastewater are solvent extraction, ion exchange, chemical precipitation, adsorption and membrane filtration. Most of these methods have many disadvantages such as; high cost, high consumption of reagents and energy, and production of a large amount of waste by-products. They are generally inefficient for treating a large volume of contaminated water which limits their uses [7,8].

Biosorption, a green process based on using natural materials from various biological sources as adsorbents recently applied worldwide due to low cost, availability, biodegradability and effectiveness in metal pollutants removal from diluted contaminated aqueous solution [8]. Other advantages of such green processes over traditional methods include faster kinetics of removal from a large volume of waste and the ability to operate over a range of

* Corresponding author.

This article was originally published with an error in the affiliation of Faten M. Abu Orabi. This version has been corrected. Please see Corrigendum in vol. 241 (2021) 361 [10.5004/dwt.2021.28053].

different conditions such as temperature and pH, along with the possibilities for metal recovery [9]. The main sources of biosorbent materials include [7,9]: nonliving biomass such as humic acid [10], microorganisms such as bacteria [11], agricultural and plant-based biomass such as leaves [12]. The last one contains various components such as pigments, polysaccharides, proteins, and phenolics. Where the functional groups in these components such as hydroxyl, carboxyl, carbonyl, sulfonate, thioether, amine, phosphate and esters provide different active sites for metal ion binding, [13,14]. Tree leaves are strong biosorbents candidates that are readily available in bulk quantities with wide diversity especially when the cost is an important parameter in choosing biosorbent materials. Also, the recovery of metal adsorbates from tree leaves can be easily accomplished by burning the loaded adsorbent followed by/or acid extraction.

Hedera helix plant is a common ornamental and medicinal plant with dense leaves. The general leaf components are cellulose, hemicelluloses, protein, lignin and starch [15], along with wide diversity of biologically active compounds such as triterpene, saponins, flavonoids, coumarins, polyacetylenes, phenolic acids, sterols and alkaloids [16].

The current study aims to characterize *H. helix* leaves as biosorbent and to determine their ability to biosorb U(VI) and Th(IV) ions for the first time. The efficiency of the biosorption process under changing different factors including dosage, temperature, initial metal concentration and time were tested. In order to understand the adsorption behavior of U(VI) and Th(IV) sorption onto *H. helix* leaves, the Langmuir, Freundlich, and Dubinin–Radushkevich models were used to model the data obtained from batch experiments. Furthermore, kinetic and thermodynamic parameters were obtained.

2. Experimental

2.1. Materials

2.1.1. Biosorbent preparation

H. helix leaves were collected from the Dahyet Al Rasheed area, North West of Amman, Jordan. The leaves were excised, washed thoroughly with tap water and then with deionized water. Leaves were air-dried for 2 d, dried at 60.0°C ± 1.0°C for 24 h and then ground to powder. The powder was passed through a sieve of 200 mesh and stored in a desiccator until used.

2.1.2. Chemicals

All reagents used in this study were of analytical grade reagents. Sodium hydroxide (NaOH) from LOBA Chemie Pvt. Ltd., Mumbai, India. Hydrochloric acid 37% (HCl) and nitric acid 69% (HNO_3) from TEDIA, Fairfield, OH, US. Sodium perchlorate ($NaClO_4$) from Acros, thorium nitrate hexahydrate ($Th(NO_3)_4{\cdot}6H_2O$) from Analar, uranyl nitrate hexahydrate ($UO_2(NO_3)2{\cdot}6H_2O$) from BDH Chemicals Ltd, Poole, England, and Arsenazo(III) indicator from Fluka, Buchs, Switzerland.

2.2. Characterization and analysis of H. helix leaves

H. helix leaves were characterized using Fourier transform infrared spectroscopy (FTIR) using a Thermo Nicolet NEXUS 670 FTIR spectrophotometer from Thermo Electron Corporation, Madison, US. X-ray diffraction (XRD) was recorded using Philips X'Pert PW 3060, from PANalytical B.V., The Netherlands, operated at 45 kV and 40 mA, thermogravimetric analysis (TGA) were carried using NETZCH STA 409 PG/PC Thermal Analyzer from NETZSCH-Geraetebau GmbH, Germany, at a heating rate of (20.0°C/min.). Micrographs of *H. helix* leaves surface was investigated by scanning electron microscope (SEM) using FEI inspect F50.

2.3. Batch experiments

The batch equilibration method has been used for the determination of the biosorption of U(VI) and Th(IV) ions by *H. helix* leaves. In a typical adsorption run, 0.1000 g of *H. helix* leaves were shaken with 25.0 mL of metal ion solution in 100 mL capped polyethylene bottles in a GFL-85 thermostatic shaker at 150 rpm and at the desired pH and temperature. At the end of the desired time, the contents of the polyethylene bottles were centrifuged for 15 min at 2,500 rpm then filtered. The filtrate was subsequently analyzed for residual concentration of the metal ion spectrophotometrically on a SpectroScan (model 80DV) at a wavelength of 650 nm for U(VI) and at 660 nm for Th(IV).

The amount of metal ion adsorbed by the *H. helix* leaves powder q_e (mg/g) was calculated using the following equation:

$$q_e = \frac{\left(C_i - C_e\right)}{m} \cdot V \tag{1}$$

where C_i: initial concentration of metal ion (mg/L), C_e: equilibrium concentration of the metal ion in solution (mg/L), V: volume of solution (L) and m: mass of *H. helix* leaves (g).

2.4. Effect of pH

The effect of pH on metal ion uptake was investigated between pH 1.0 and 5.0 under continuous shaking of 25.0 mL of metal ion solution with 0.1000 g of solid *H. helix* leaves for a fixed contact time of 24 h at 25.0°C. Higher pH values are not considered because precipitation of the metal cations as insoluble hydroxides could occur and interfere with adsorption [17].

2.5. Kinetic studies

Experiments for the determination of the equilibrium time for the adsorption process was studied by shaking 0.1000 g of the *H. helix* leaves with 25.0 mL of 30 mg/L metal ion solution at pH 3.0 for both U(VI) and Th(IV), over a time period of 0.25–72 h following the procedure of batch experiment using separate samples over the different times. Two kinetic models pseudo-first-order model and pseudo-second-order model were applied to predict the adsorption kinetics.

The linear form of the pseudo-first-order model is expressed as follows:

$$\ln\left(q_e - q_t\right) = \ln q_e - k_1 t \tag{2}$$

The integrated linear form of pseudo-second-order model:

$$\frac{t}{q_t} = \frac{1}{k_2 q_e^2} + \frac{t}{q_e} \tag{3}$$

where k_1 = pseudo-first-order adsorption rate constant (min^{-1}), k_2 = pseudo-second-order adsorption rate constant (g/mg min). q_e = amount of metal ions adsorbed per unit mass of adsorbent at equilibrium (mg/g) and q_t = amount of metal ions adsorbed per unit mass at time t (mg/g) [18].

2.6. Biosorption isotherms

Langmuir, Freundlich and Dubinin–Radushkevich [19–21] models were tested using the results obtained from the biosorption of U(VI) and Th(IV) ions by *H. helix* leaves. A 25.0 mL from each metal ion solution with different initial concentrations C_i (10, 20, 30, 40, 50 ppm) were added separately to polyethylene bottles containing 0.1000g of *H. helix* leaves following the procedure of the batch experiment, all samples were shaken for 24 h at different temperatures (25.0°C, 35.0°C and 45.0°C).

The following equations were used to obtain the different parameters:

Langmuir equation:

$$\frac{1}{q_e} = \left(\frac{1}{K_L q_m}\right)\frac{1}{C_e} + \frac{1}{q_m} \quad \text{(Form II)} \tag{4}$$

Freundlich equation:

$$\log q_e = \log K_F + \frac{1}{n}\log C_e \tag{5}$$

Dubinin–Radushkevich equation:

$$\ln q_e = \ln q_{\max} - \beta\varepsilon^2 \tag{6}$$

where ε, the Polanyi potential, is defined by the following relationship:

$$\varepsilon = RT \ln\left(1 + \frac{1}{C_{eq}}\right) \tag{7}$$

2.7. Desorption studies

The desorption of U(VI) and Th(IV), separately, from loaded *H. helix* leaves, was carried using the batch method. Batch experiments for U(VI) and Th(IV) loading were applied as follows: 50.0 mL of 2,000 ppm of each metal ion were added to 4.0000 g of *H. helix* leaves, separately. All samples were shaken for 24 h at 25.0°C. The concentration of the metal ion remaining in the solution was determined by a UV-Vis spectrophotometer. The loaded powder was washed, air dried, then dried at 60.0°C for 24 h.

The desorption of U(VI) and Th(IV), separately, from loaded *H. helix* leaves was carried using the batch method. For desorption experiments, 10.0 mL of the desorbing agent was added to 0.1000 g of the loaded *H. helix* leaves in a centrifuge tube and shaken in a GFL-85 thermostatic shaker at 150 rpm for 1 h at room temperature. The solution was then centrifuged and the supernatant was collected for further analysis to examine the concentration of loaded metal desorbed from the *H. helix* leaves powder by UV-Vis spectrophotometer. On the same sample, the desorption procedure was repeated four times, each one with new fresh 10.0 mL of nitric acid (0.10 M and 1.0 M) as a desorbing agent. Each measurement was repeated two times to make sure of the accuracy and reproducibility of the results, then the average was taken.

3. Results and discussion

3.1. Characterization of H. helix leaves

3.1.1. FTIR analysis

H. helix leaves were analyzed by FTIR spectroscopy for major functional groups existing. Fig. 1 illustrates the spectra over the range 400–4,000 cm^{-1}.

Fig. 1 shows the following characteristic peaks. Within the range of the OH and NH stretching vibrations, a broadband observed at 3,324 cm^{-1} corresponds to the free hydroxyl groups and bonded O–H of carboxylic acids, and to the –NH groups. The peak at 2,913 cm^{-1} is due to the asymmetric stretching vibration of saturated aliphatic hydrocarbon chains (C–H) in methyl ($–CH_3$) and methylene ($–CH_2–$) groups, and the peak at 2,854 cm^{-1} to C–H symmetric stretching of methylene in aliphatic chains in cellulose and to asymmetric stretching of CH_3 of methoxy group in lignin. The peak at 1,726 cm^{-1} corresponds to carbonyl groups stretching in carboxyl (–COOH) and ester (–COOR) groups, as in hemicelluloses. The peak at 1,604 cm^{-1} assigned to asymmetric and symmetric stretching vibrations of C–O in ionic carboxylic groups ($–COO^-$), The peak at 1,372 cm^{-1} may be assigned to the symmetric stretching formation of –OH of carboxylic acids and phenols, which is also assigned to the symmetric bending stretching of CH_3 indicating the presence of lignin [22–25]. The peak at 1,314 was assigned for C–O stretch in cellulose while the peak at 1,236 cm^{-1} was assigned for acetyls groups of hemicellulose [22]. Finally, the peak around 1,017 cm^{-1} may be assigned for C–C, C–OH, C–O–C, C–H and side group vibrations of cellulose and lignin. FTIR spectrum of *H. helix* leaves agrees with those of lignocellulose materials published in the literature [26].

The absorbance spectrum of *H. helix* leaves after loaded with U(IV) and Th(VI) is shown in Fig. 2. After the biosorption of uranium and thorium, the spectrum was changed a little compared with that before. It was just shifted, with no new bands appeared. This indicates that the structure of *H. helix* leaves had not changed after metal adsorption, After biosorption of uranium and thorium, the broadband at 3,324 cm^{-1} weakened which indicated that amino and hydroxyl groups participated in the binding of U(VI) and Th(IV). The peaks at 1,604 and 1,372 cm^{-1} were shifted to 1,615 and 1,369 cm^{-1} after uranium adsorption, and shifted to 1,616 and 1,369 cm^{-1} after thorium adsorption, respectively. This suggested that after the adsorption of uranium and thorium, some combinations of H^+ were replaced by U(VI) and Th(IV). These results suggest that the amino, hydroxyl and carbonyl were involved in the mechanism of adsorption of uranium and thorium with the *H. helix* leaves.

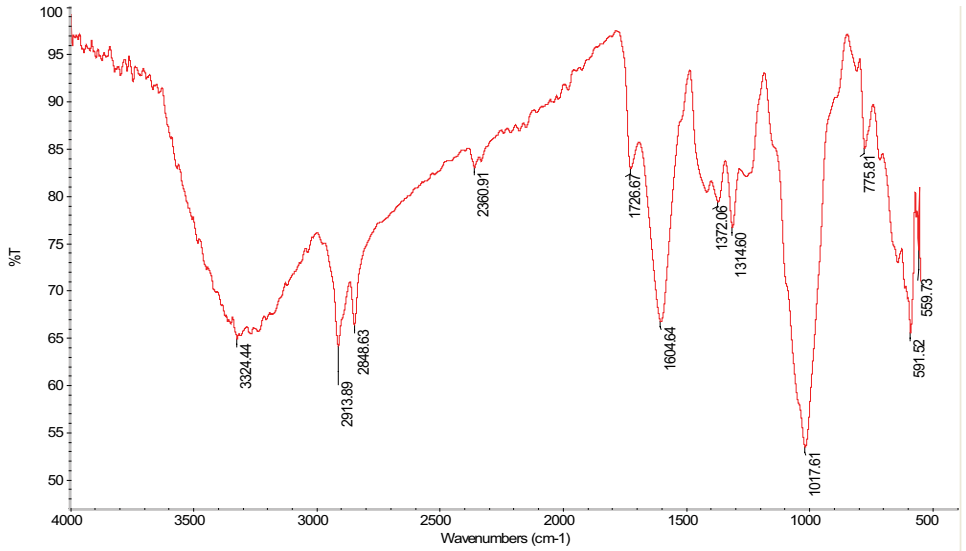

Fig. 1. FTIR for *Hedera helix* leaves.

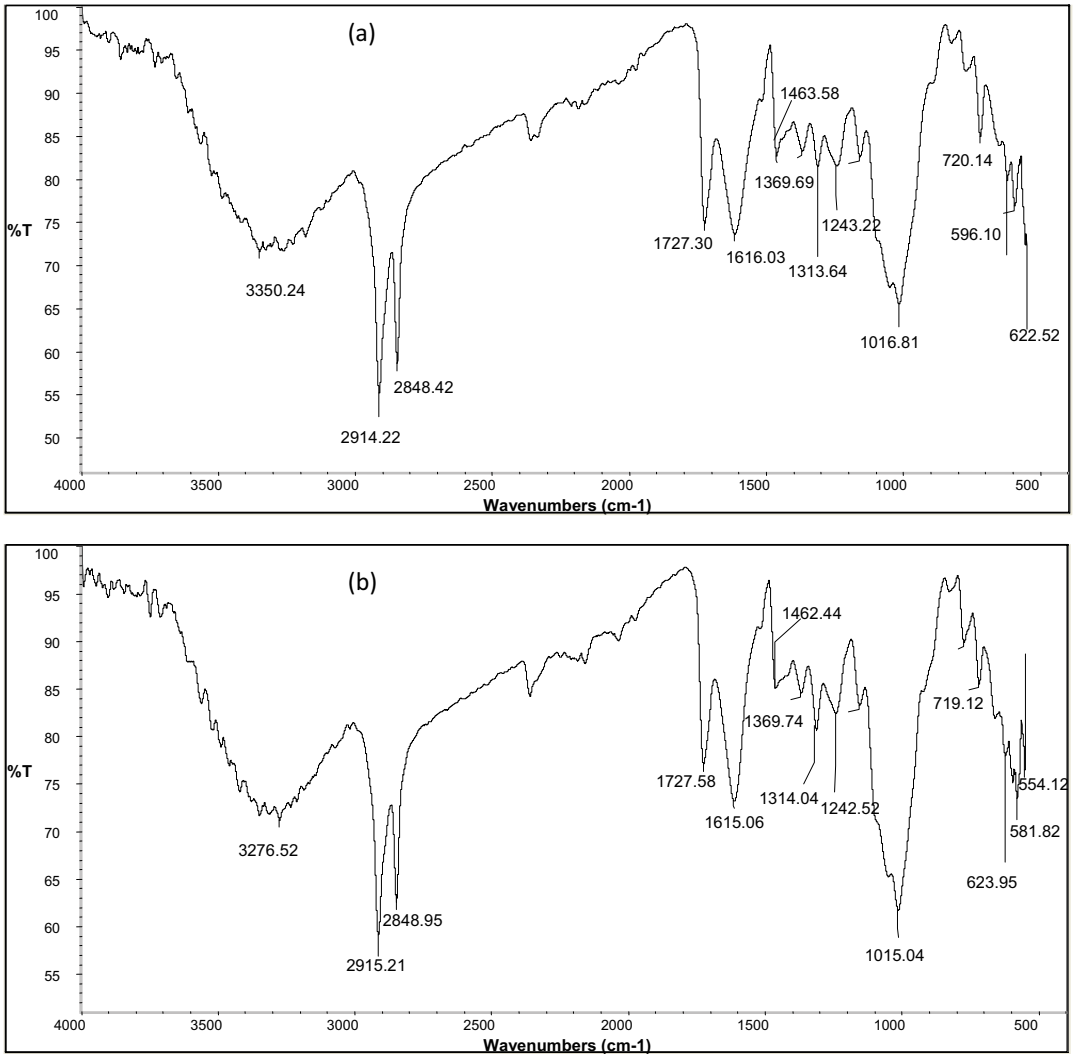

Fig. 2. FTIR for *Hedera helix* leaves (a) after adsorption of uranium and (b) after adsorption of thorium.

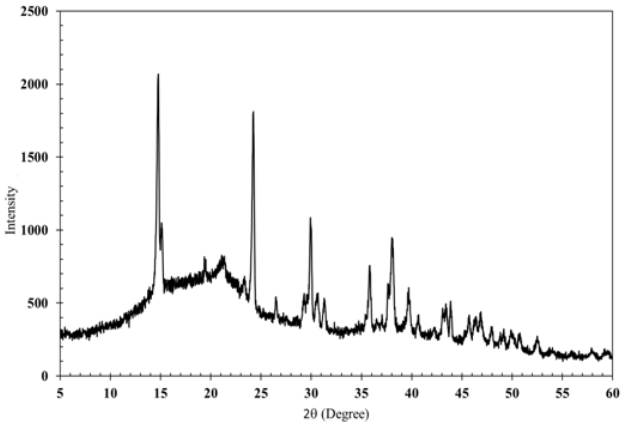

Fig. 3. XRD pattern of *Hedera helix* leaves.

It is well indicated from the FTIR spectrum of *H. helix* leaves that carboxyl and hydroxyl groups were present in abundance. The biosorption of U(VI) and Th(IV) on the *H. helix* leaves could be due to the electrostatic attraction between these groups and U(VI) and Th(IV) ions, this suggested that ion exchange was one of the main biosorption mechanisms.

3.1.2. XRD characterization

The XRD pattern (Fig. 3) shows a typical spectrum of cellulosic material which had main and secondary peaks at 2θ = 14.78 and 24.24. The main peak indicates the presence of crystalline cellulose while the second peak corresponds to less crystalline polysaccharide structure. The peak at 2θ = 35.8 is assigned to hemicelluloses and the strong main peaks at 2θ = 14.78, 29.9 and 37.5 correspond to lignin [24,25].

3.1.3. Thermogravimetric analysis

The thermal stability of the *H. helix* leaves was investigated under dry nitrogen atmosphere by TGA as shown in Fig. 4.

The TGA thermogram shows three main regions during the thermal decomposition of the *H. helix* leaves. The first region of weight loss measured at (T < 150°C) was 6.69%, and mainly corresponds to evaporation of adsorbed water, and some small volatile organic molecules like oils, dyes, etc [24]. The second region corresponds to the decomposition of the biomass of *H. helix* leaves at a temperature between 150°C and 500°C with 62.49% weight loss, and the third decomposition step corresponds to the oxidation of the charred residue at T > 500°C with 7.68% weight loss, similar results were obtained by Garcia-Maraver et al. [27] for biomass from olive trees.

3.1.4. Scanning electron microscope

The surface topography and bulk structure of free *H. helix* leaves were observed by SEM (Fig. 5). The *H. helix* leaves have an irregular, heterogeneous and porous surface with flakes and plate type providing a large number of adsorption sites. Also, SEM images show interspaces within the free *H. helix* leaves powder which increases the surface area. It has been suggested that such surface topography providing channels and space for metal sorption [28].

3.2. Effect of pH

One of the most important parameters in any biosorption process is solution pH. It affects the activity of the different functional groups existing in the biosorbent which are involved in metal ions binding and also affects the speciation of metallic ions in the aqueous solution [17].

The effect of pH on the biosorption of uranium by *H. helix* leaves shows that as the pH increases (from 1.0 to 3.0), uranium loading increased with a maximum occurring at pH 3.0, and stayed constant until pH 5.0. The results are presented in Fig. 6. At strongly acidic conditions (pH 1.0) minimum, biosorption of uranium ions by *H. helix* leaves was observed because, at high proton concentration, protons are preferentially adsorbed on the adsorbent rather than the U(VI) ions, and the binding sites became positively charged repelling positive ions [24,26].

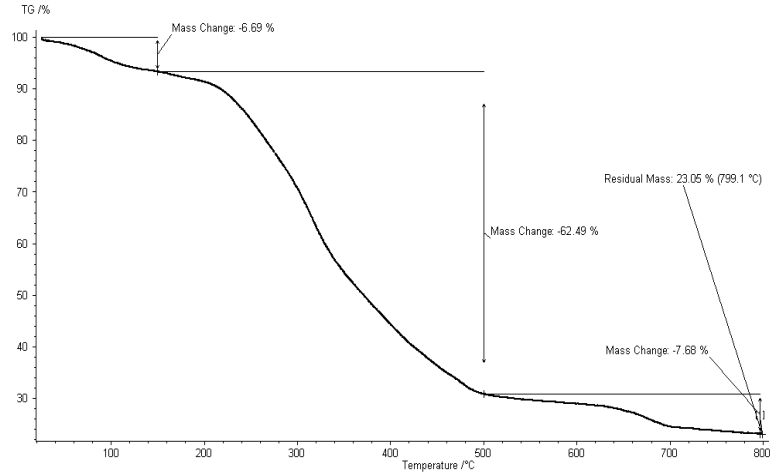

Fig. 4. TGA for *Hedera helix* leaves.

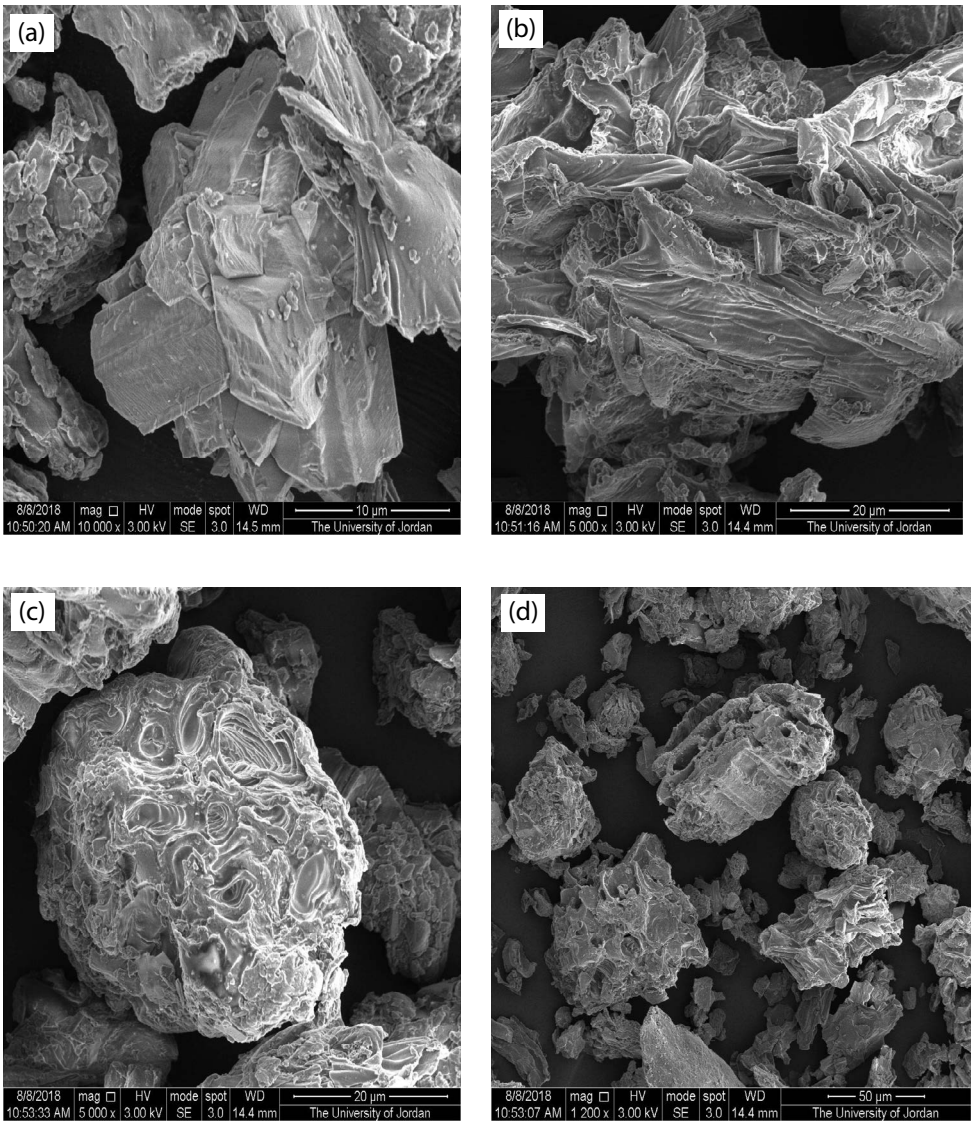

Fig. 5. SEM micrographs for free *Hedera helix* leaves at different magnifications (a) 10,000x, (b) 5,000x, (c) 5,000x and (c) 1,200x.

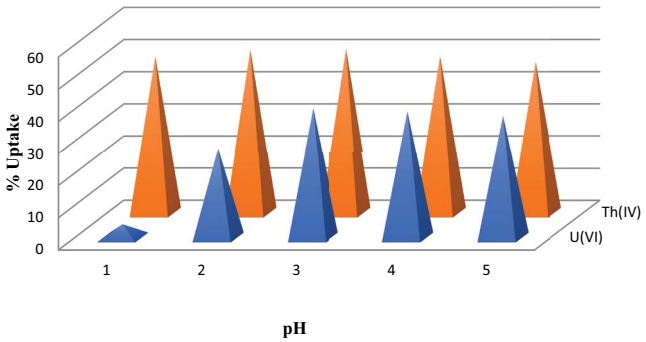

Fig. 6. Effect of pH on U(VI) and Th(IV) biosorption onto *Hedera helix* leaves at 25.0°C.

As pH increases different hydrolyzed forms of uranium will exist, the following ionic species exist at pH > 3.0 up to near neutral: UO_2^{2+}, $[UO_2(OH)]^+$, $[(UO_2)_2(OH)_2]^{2+}$, $[(UO_2)_3(OH)_5]^+$, Fig. 7. The predominant species of uranium that exists at pH ≤ 4.3 are the monomeric species UO_2^{2+}, with small amounts of $[UO_2(OH)]^+$, and at higher pH, precipitation starts due to the formation of insoluble complexes in aqueous solution and adsorption decreases [29,30]. Thus, pH 3.0 was chosen for further experiments, where maximum adsorption associated with UO_2^{2+} ions is observed.

As shown in Fig. 6, the sorption efficiency of Th(IV) onto *H. helix* leaves powder did not have considerable change with varying pH from 1.0 to 5.0, with maximum adsorption occurs at pH 3.0. Thus, pH 3.0 was chosen for further experiments. The very small variation in the Th(IV) adsorption over the studied pH range indicates intense interactions of Th(IV) ions to the *H. helix* leaves surface, where Th(IV) is a hard cation with a high oxidation state [32]. Thorium occurs exclusively in aqueous solution especially in an acidic medium as stable tetra positive aqua ion $[Th(H_2O)_9]^{4+}$ especially at pH 3.0 or less. At higher pH the following species exist, $[Th(OH)_3]^+$ at pH (3.0–5.0), $[Th(OH)_2]^{2+}$ at pH (4.5–5.5), and $Th(OH)_4$ at pH > 6.0 [33], Fig. 8.

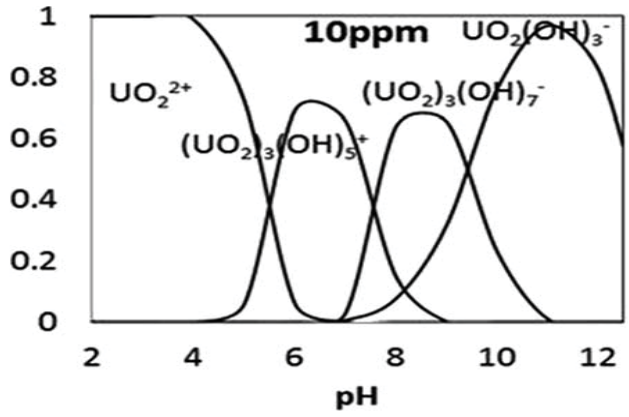

Fig. 7. Distribution of uranyl species in solution as a function of pH (Figure taken from reference [31]).

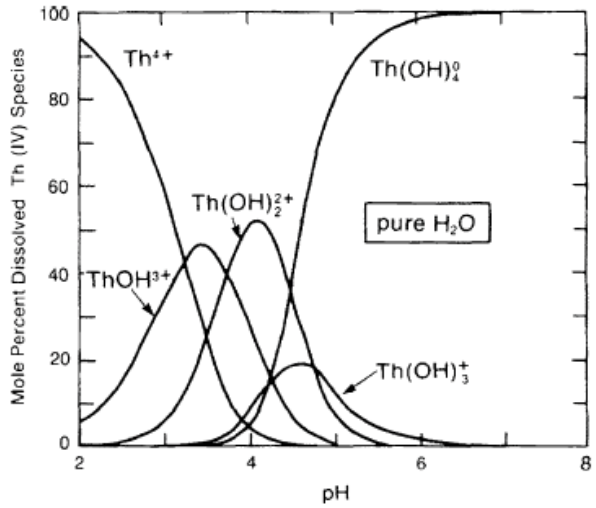

Fig. 8. Distribution of thorium species as a function of pH (Figure taken from reference [34]).

The optimum pH for U(VI) and Th(IV) was 3.0. This range of pH (3.0–4.0) is in the range of pKa of the carboxyl groups on the biomass surface which indicates that one of the functional groups on the biomass responsible for the metal binding is the carboxyl group [35].

3.3. Effect of adsorbent dosage

Effect of adsorbent dose of *H. helix* leaves on biosorption has been studied by using a 30 ppm concentration of U(VI) and Th(IV) solutions separately, with different doses (0.1000–0.5000 g) of *H. helix* leaves powder under continuous shaking for a fixed contact time of 24 h at 25.0°C and pH 3.0 (Fig. 9).

From Fig. 9, the removal efficiency of U(VI) and Th(IV) increases with an increase in the biosorbent dosage as long as the biosorbent is not saturated. This is due to the higher number of active sites available for adsorption. However, with the increase of biomass, a 'screen' occurs on the adsorbent surface due to partial aggregation of

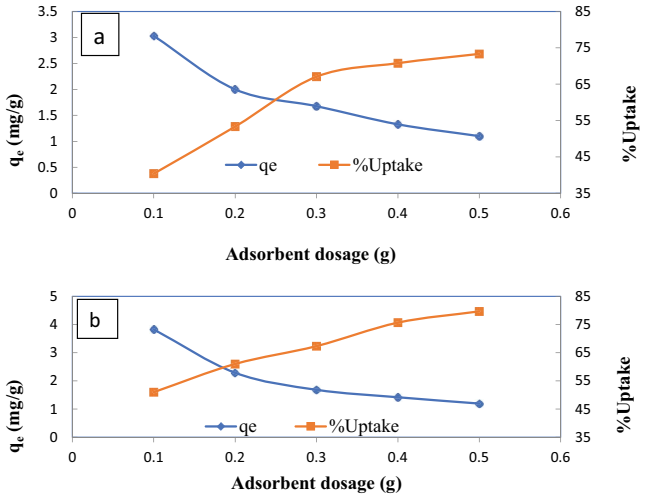

Fig. 9. Effect of adsorbent dosage on the adsorption of (a) U(VI) and (b) Th(IV) onto *Hedera helix* leaves (initial concentration 30 ppm, pH 3.0 and 25.0°C).

biomass, which protects the binding sites and decreases the effective surface area existing for adsorption; results in decreasing the amount of adsorption per unit weight of the adsorbent (q_e) [28]. For further work, an adsorbent weight of 0.1000 g (in 25.0 mL metal ion solution) is adequate for the optimal removal of all metal ions under study. Similar results were observed by Parab et al. [36] using coir pith for uranium(VI) uptake.

3.4. Effect of temperature

The effect of changing temperature (25°C, 35°C, and 45°C) on sorption of U(VI) and Th(IV) by *H. helix* leaves was studied. Fig. 10 shows a direct relationship between temperature and percentage uptake of U(VI) and Th(IV) ions, increase temperature enhance U(VI) and Th(IV) uptake by *H. helix* leaves which indicated that the biosorption mechanism is controlled by an endothermic reaction. This may indicate that some new active sites are generated during heating or that the ions overcome the energy barrier to resist concentration gradient or endure diffusion transmission [17,26].

3.5. Effect of contact time and sorption kinetic models

The plots of uptake vs. time for U(VI) and Th(IV) by *H. helix* leaves are shown in Fig. 11. Since the variation in the %uptake values after 24 h was very small. So 24 h as shaken time was chosen for all further experiments at pH 3.0 for U(VI) and Th(IV).

The adsorption speed consisted of two stages: the fast stage within the first 15 min, then the adsorption speed slowed down gradually as equilibrium approached within 24 h. Such two stages are common in most adsorption systems, where the adsorbent contains a large number of active binding sites for metal binding at the first stage of the adsorption process. As time increases, a saturation of these binding sites is reached and the adsorption capacity decreases [37].

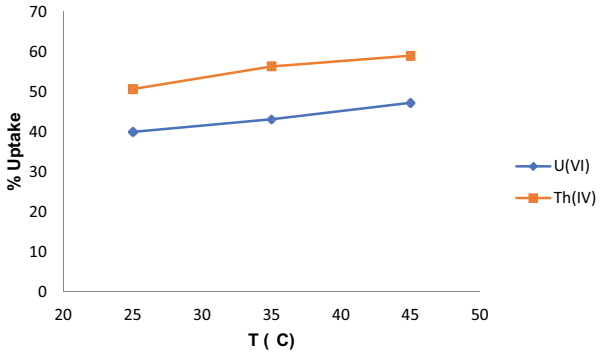

Fig. 10. %Uptake of U(VI) and Th(IV) by *Hedera helix* leaves at different temperatures (pH 3.0, 25.0°C, initial concentration 30 ppm and adsorbent dosage 0.1000 g/25.0 mL).

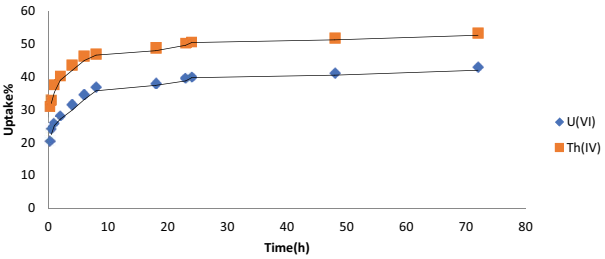

Fig. 11. %Uptake of U(VI) and Th(IV) by *Hedera helix* leaves with time at pH 3.0 and 25.0°C.

Correlation coefficients, R^2, obtained from pseudo-second-order model are higher than that obtained from pseudo-first-order model, also q_e experimental agrees with q_e calculated from the pseudo-second-order kinetic model rather than calculated from pseudo-first-order model. Therefore, the biosorption process by *H. helix* leaves follows the pseudo-second-order kinetic model (Fig. 12) and the results are presented in Table 1.

3.6. Effect of initial concentration

The percentage of U(VI) and Th(IV) uptake by *H. helix* leaves powder decreased with increasing initial concentration (10, 20, 30, 40, and 50 ppm) and the variation was from 69.4% to 27.9% for U(VI), and from 79.0% to 36.6% for Th(IV) at 25.0°C. However, the uptake rate was over 70% for the lowest initial metal ions concentration (10 ppm), which

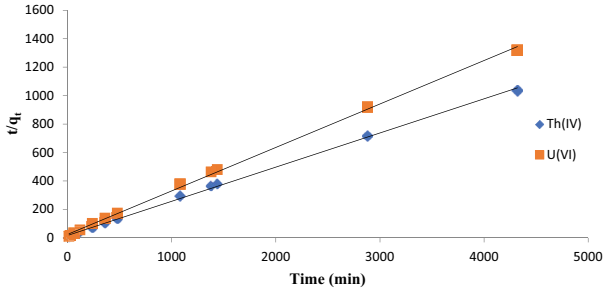

Fig. 12. Pseudo-second-order sorption kinetics of U(VI) and Th(IV) by *Hedera helix* leaves at pH 3.0, 25.0°C, initial concentration 30 ppm and adsorbent dosage 0.1000 g/25.0 mL.

means that *H. helix* leaves powder has a high adsorption affinity to the low concentration of the metal ions. This can be interpreted by the fact that at low concentrations, the ions contact with the adsorbent sufficiently, and all of the ions can interact with the *H. helix* leaves. While the amount of adsorption per unit weight of the adsorbent (q_e) increased with increasing of the initial metal ions concentrations at the range of the experimental concentration.

3.7. Adsorption isotherms

The adsorption isotherm is the primary source of information on the adsorption process and forms an important tool in designing the adsorption system, express adsorbents capacities and surface properties, and for optimization mechanism pathways of the adsorption process [38]. The biosorption by *H. helix* leaves experiments were carried out by shaking a suspension of 0.1000 g *H. helix* leaves in 25.0 mL of metal ion solutions of different concentrations ranging from 10 to 50 ppm at pH 3.0 for each metal ion for 24 h. Fig. 13 shows the biosorption capacities (q_e) vs. (C_e).

Experimental data of adsorption isotherms are well described by different models, such as Langmuir, Freundlich, and Dubinin–Radushkevich models. The results are summarized in Table 2.

As seen from Table 2, the R^2 values for Langmuir and Freundlich models are very high. A possible explanation is that the surface of *H. helix* leaves is a mixture of homogeneous and heterogeneous sites, the biosorbents involve various building blocks that are consist of diverse molecules, which display various binding sites [39]. This suggests that the biosorption of metal ions on *H. helix* leaves

Table 1
Parameters of pseudo-first-order and pseudo-second-order kinetic models of U(VI) and Th(IV) biosorption by *Hedera helix* leaves at pH 3.0 and 25.0°C

Parameters	U(VI)		Th(IV)	
	Pseudo-first-order	Pseudo-second-order	Pseudo-first-order	Pseudo-second-order
R^2	0.886	0.998	0.991	0.998
q_e (mg/g) calculated	1.17	3.29	1.28	4.17
q_e (mg/g) experimental	3.28	3.28	4.18	4.18
k_2 (g/mg min) × 10^{-3}	–	3.76	–	3.44

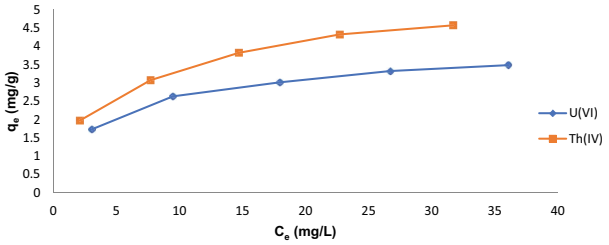

Fig. 13. Adsorption isotherm of U(VI) or Th(IV) with *Hedera helix* leaves at pH 3.0 and 25.0°C.

surface is complex, involving more than one mechanism. Similar observations have been reported by Zou et al. [24] for uranium biosorption on grapefruit peel; by Parab et al. [36] for uranium biosorption using coir pith. The R_L values obtained from Langmuir parameters for U(VI) are between 0.078 to 0.059 and between 0.081 to 0.065 for Th(IV). All R_L values are between 0 and 1, suggesting that the adsorption process of metal ions by *H. helix* leaves is favorable.

Also, the values of the constant n calculated from the Freundlich model were always greater than 2; indicating that the adsorption of U(VI), and Th(IV) by *H. helix* leaves is favorable. The Langmuir and Freundlich constants (K_L, q_m and K_F) increased with increasing temperature, these results indicated that U(VI) and Th(IV) ions can be easily removed by *H. helix* leaves from aqueous solutions.

The maximum U(VI) or Th(IV) ions biosorption capacities, q_m, of the present study are compared with the other agricultural adsorbents reported in the literature (Table 3). The results indicate that *H. helix* leaves show good sorption capacity compared to the other agricultural adsorbents, however, such comparison between different adsorbents materials is not accurate, due to different experimental conditions applied such as the adsorbent mass used, the volume of metal ion solution and the initial concentration of metal ion that affect the value of q_m.

The magnitude of E from Dubinin–Radushkevich isotherms for U(VI) and Th(IV) adsorbed onto *H. helix* leaves are less than 8 kJ/mol (Table 2), which is indicating that physical forces may affect the adsorption process [43].

3.6.1. Thermodynamics of biosorption by H. helix leaves

In order to understand the biosorption involved in the removal process, thermodynamic parameters of the system, including changes in Gibbs free energy ($\Delta G°$), change in enthalpy of adsorption ($\Delta H°$) and changes in the entropy of adsorption ($\Delta S°$), were calculated using the following equations:

$$\Delta G° = -RT \ln K_d \tag{8}$$

$$\ln K_d = \frac{\Delta S°}{R} - \frac{\Delta H°}{RT} \tag{9}$$

Table 2
Langmuir, Freundlich and Dubinin–Radushkevich isotherm parameters for biosorption of U(VI) and Th(IV) by *Hedera helix* leaves at different temperatures

T (°C)	Langmuir isotherm				Freundlich isotherm			Dubinin–Radushkevich			
	R^2	q_m (mg/g)	K_L (L/mg)	R_L	R^2	n (L/mg)	K_F (mg/g)	R^2	β (mol²/kJ²)	q_m (mg/g)	E (kJ/mol)
U(VI)											
25.0	0.998	3.86	0.23	0.08	0.979	3.53	1.31	0.918	1.28	3.20	0.63
35.0	0.992	4.24	0.25	0.07	0.960	3.62	1.49	0.905	0.92	3.49	0.74
45.0	0.994	4.46	0.32	0.06	0.972	3.75	1.69	0.881	0.59	3.74	0.92
Th(IV)											
25.0	0.995	5.16	0.23	0.08	0.994	3.15	1.58	0.861	0.79	4.03	0.80
35.0	0.997	5.56	0.28	0.07	0.986	3.21	1.82	0.882	0.55	4.42	0.95
45.0	0.989	5.92	0.29	0.07	0.994	3.39	2.03	0.845	0.34	4.61	1.22

Table 3
Comparison of the sorption capacity for U(VI) and Th(IV) by various agricultural waste biomass

Metal ion	Biosorbent	q_{max} (mg/g)	Optimum pH	Reference
U(VI)	Rice husk	14.86	3.0	[17]
	Orange peel	16.12	4.0	[40]
	Poplar leaf	2.30	4.0	[41]
	Poplar ranches	0.40	4.0	
	Hedera helix leaves	3.86	3.0	This study
Th(IV)	Rice husk	24.08	4.0	[42]
	Hedera helix leaves	5.16	3.0	This study

The K_d (distribution coefficient) was calculated from the intercept of $\ln(q_e/C_e)$ vs. q_e, values of K_d are summarized in Table 4. Results showed that K_d increases as the temperature increases. These results indicated the endothermic nature of adsorption of U(VI) or Th(IV) onto *H. helix* leaves powder. The values of enthalpy ($\Delta H°$) and entropy ($\Delta S°$) were obtained from the slope and the intercept of the plot of $\ln K_d$ vs. $1/T$ for each metal ion (Fig. 14), respectively, while $\Delta G°$ was calculated at 25.0°C using equation 1.2. The results are shown in Table 5.

Gibb's free energy indicates the spontaneous nature of the adsorption process; where a more negative value of $\Delta G°$ reflects more energetically favorable metal adsorption onto the adsorbent [17,43]. The negative values of $\Delta G°$ obtained in this study for *H. helix* leaves indicate that the adsorption of each metal ion is favorable and the process is spontaneous as shown in Table 5. Positive values of enthalpy change $\Delta H°$ indicate the endothermic nature of the adsorptions of metal ions by *H. helix* leaves. A possible explanation of the endothermic nature of the enthalpy of adsorption is stated by Alkaram et al. [44] as follows: "The endothermic enthalpy gives a clear indication of strong interaction between adsorbate and adsorbent. This can be explained by the fact that each molecule of adsorbate has to displace more than one molecule of solvent. This dehydration process of ions requires energy" (adapted from Alkaram et al. [44]) In other words U(VI) and Th(IV) ions are well solvated and in order for each metal ions to be adsorbed on the *H. helix* leaves surface they have to lose part of their hydration sphere, this dehydration requires energy and this energy supersedes the exothermicity of the ions getting attached to the surface [43].

The positive values of $\Delta S°$ indicate increased randomness at the solid/solution interface during the adsorption process, which was the driving force for adsorption. Such positive entropy of adsorption reflects the affinity of the *H. helix* leaves toward the metal ions. A possible explanation is that the adsorbed water molecules on the *H. helix* leaves surface, which is displaced by the metal ions, gain more translational energy than is lost by the adsorbed metal ions, thus increasing the randomness of the system. Also, the dehydration of metal ions increases the randomness of the system. The increase in the adsorption capacity of adsorbents at higher temperatures may be due to the strong interaction between adsorbate and adsorbent [10].

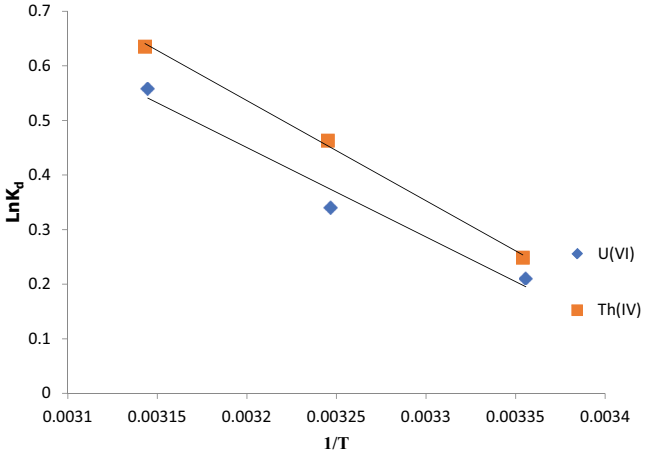

Fig. 14. Plots of $\ln K_d$ vs. $1/T$ at pH 3.0 and 25.0°C.

Table 4
Distribution coefficient of adsorption of U(VI) and Th(IV) onto *Hedera helix* leaves at different temperatures

Metal ion	T (°C)	K_d	$\ln K_d$
U(VI)	25.0	1.235	0.211
	35.0	1.406	0.341
	45.0	1.747	0.558
Th(IV)	25.0	1.283	0.249
	35.0	1.589	0.463
	45.0	1.889	0.636

3.7. Desorption experiments

In order to estimate the reversibility of U(VI) or Th(IV) sorption onto *H. helix* leaves, desorption experiments using 1.0 or 0.1 M HNO_3 of nitric acid as a desorption solution were performed. The maximum desorption of U(VI) or Th(IV) from *H. helix* leaves was observed using 0.1 M HNO_3 within the first stage of desorption (Table 6). The %Recovery was decreased continuously with increasing the recovery stages for both metal ions by the two concentrations of the desorption reagent (HNO_3). The best percent recovery of U(VI) loaded on *H. helix* leaves was obtained when 0.1 M HNO_3 was used, while that of Th(IV) loaded on *H. helix* leaves was obtained when 1.0 M HNO_3 as shown by the cumulative percent after four recovery stages.

From the results of U(VI) and Th(IV) desorbed from loaded *H. helix* leaves the fraction of adsorbed metal ions that were not recovered by the desorption reagents (incomplete desorption), probably represents metal ions that are strongly adsorbed onto *H. helix* leaves powder through various complex mechanisms [45].

4. Conclusions

H. helix leaves are cheap and easily available material that can be used as a low-cost and biodegradable adsorbent for U(VI) and Th(IV) removal from aqueous solutions. The biosorption of U(VI) and Th(VI) by *H. helix* leaves was investigated by batch technique. Performances of biosorption process are strongly affected by pH, temperature, contact time, initial U(VI) and Th(IV) concentration and *H. helix* leave dose. The biosorption followed the pseudo-second-order kinetic model and the obtained

Table 5
Thermodynamic parameters for biosorption of U(VI) and Th(IV) by *Hedera helix* leaves at 25.0°C

Metal ion	$\Delta G°$ (kJ/mol)	$\Delta H°$ (kJ/mol)	$\Delta S°$ (J/mol K)
U(VI)	–0.52	13.62	47.33
Th(IV)	–0.62	15.27	53.31

Table 6
Desorption (%Recovery) of U(VI) or Th(IV) loaded onto *Hedera helix* leaves

U(VI)			Th(IV)		
Recovery stage	%Recovery by 1.0 M HNO_3	%Recovery by 0.1 M HNO_3	Recovery stage	%Recovery by 1.0 M HNO_3	%Recovery by 0.1 M HNO_3
First 10.0 mL	45	53.9	First 10.0 mL	17.9	37.5
Second 10.0 mL	12.6	15.3	Second 10.0 mL	16.5	6.6
Third 10.0 mL	3.6	4.0	Third 10.0 mL	13.4	4.3
Fourth 10.0 mL	1.5	2.2	Fourth 10.0 mL	10.0	1.2
%Cumulative recovery	62.7	75.4	%Cumulative recovery	87.8	49.6

biosorption equilibrium data fitting very well with Langmuir and Freundlich adsorption isotherms. The thermodynamic parameters obtained showed that the adsorption processes of U(VI) or Th(IV) ions by *H. helix* leaves are favorable and spontaneous, and the biosorption by *H. helix* leaves is an endothermic process and entropy-driven for both U(VI) and Th(IV) ions. The highest percent cumulative recovery for U(VI) was achieved using 0.1 M HNO_3 (~75%), while for Th(IV) it was achieved using 1.0 M HNO_3 (~88%), after four recovery stages, for both metal ions.

References

[1] A. Kausar, H. Bhatti, Adsorptive removal of uranium from wastewater: a review, J. Chem. Soc. Pak., 35 (2013) 1041–1052.
[2] J. Al-Jundi, E. Werner, P. Roth, V. Hollriegl, I. Wendler, P. Schramel, Thorium and uranium contents in human urine: influence of age and residential area, J. Environ. Radioact., 71 (2004) 61–70.
[3] G. Choppin, Actinide speciation in the environment, Radiochim. Acta, 91 (2003) 645–649.
[4] J. Lloyd, J. Renshaw, Bioremediation of radioactive waste: radionuclide–microbe interactions in laboratory and field-scale studies, Curr. Opin. Biotechnol., 16 (2005) 254–260.
[5] F. Khalili, A. Khalifa, G. Al-Banna, Removal of uranium(VI) and thorium(IV) by insolubilized humic acid originated from Azraq soil in Jordan, J. Radioanal. Nucl. Chem., 311 (2017) 1375–1392.
[6] S. Seyhan, M. Merdivan, N. Demirel, Use of o-phenylene dioxydiacetic acid impregnated in Amberlite XAD resin for separation and preconcentration of uranium(VI) and thorium(IV), J. Hazard. Mater., 152 (2008) 79–84.
[7] F. Fu, Q. Wang, Removal of heavy metal ions from wastewaters: a review, J. Environ. Manage., 92 (2011) 407–418.
[8] H. Alluri, S. Ronda, V. Settalluri, J. Bondili, V. Suryanarayana, P. Venkateshwar, Biosorption: an eco-friendly alternative for heavy metal removal, Rev. Afr. J. Biotechnol., 6 (2007) 2924–2931.
[9] V. Gupta, A. Nayak, S. Agarwal, Bioadsorbents for remediation of heavy metals: current status and their future prospects, Environ. Eng. Res., 20 (2015) 1–18.
[10] F. Khalili, G. Al-Banna, Adsorption of uranium(VI) and thorium(IV) by insolubilized humic acid from Ajloun soil – Jordan, J. Environ. Radioact., 146 (2015) 16–26.
[11] R. Vieira, B. Volesky, Biosorption: a solution to pollution?, Int. Microbial., 3 (2000) 17–24.
[12] M. Aoyama, M. Tsuda, N. Cho, S. Doi, Adsorption of trivalent chromium from dilute solution by conifer leaves, Wood Sci. Technol., 34 (2000) 55–63.
[13] S. Doyurum, A. Celik, Pb(II) and Cd(II) removal from aqueous solutions by olive cake, J. Hazard. Mater. B, 138 (2006) 22–28.
[14] S. Qaiser, A. Saleemi, M. Ahmad, Heavy metal uptake by agro based waste materials, Electron. J. Biotechnol., 10 (2007) 409–416.
[15] F. Baret, T. Fourty, Estimation of leaf water content and specific leaf weight from reflectance and transmittance measurements. Agronomie, EDP Sciences, 17 (1997) 455–464.
[16] Y. Lutsenko, W. Bylka, I. Matlawska, R. Darmohray, *Hedera helix* as a medicinal plant, Herba Polonica, 56 (2010) 83–96.
[17] L. Xia, R. Li, Y. Xiao, W. Zheng, K. Tan, Removal of uranium(VI) from aqueous solution by rice husk, Environ. Prot. Eng., 43 (2017) 41–53.
[18] H. Qiu, L. Lv, B. Pan, Q. Zhang, W. Zhang, Q. Zhang, Critical review in adsorption kinetic models, J. Zhejiang Univ. Sci. A, 10 (2009) 716–724.
[19] I. Langmuir, The adsorption of gases on plane surfaces of glass, mica, and platinum, J. Am. Chem. Soc., 40 (1918) 1361–1403.
[20] H.M.F. Freundlich, Over the adsorption in solution, J. Phys. Chem., 57 (1906) 385–471.
[21] M.M. Dubinin, L.V. Radushkevich, The Equation of the Characteristic Curve of Activated Charcoal, Proceedings of the Academy of Sciences, Physical Chemistry Section, 55 (1947) 331.
[22] N.S.M. Md Yunos, A.S. Baharuddin, K.F. Md Yunos, M. Nazli Naim, H. Nishida, Physicochemical property changes of oil palm mesocarp fibers treated with high-pressure steam, BioResources, 7 (2012) 5983–5994.
[23] M. Torab-Mostaedi, Biosorption of lanthanum and cerium from aqueous solutions using tangerine (*Citrus reticulata*) peel: equilibrium, kinetic, and thermodynamic studies, Chem. Ind. Chem. Eng. Q, 19 (2013) 79–88.
[24] W. Zou, L. Zhao, L. Zhu, Efficient uranium(VI) biosorption on grapefruit peel: kinetic study and thermodynamic parameters, J. Radioanal. Nucl. Chem., 292 (2012) 1303–1315.
[25] S. Nanda, P. Mohanty, K. Pant, S. Naik, J. Kozinski, A. Dalai, Characterization of North American lignocellulosic biomass and biochars in terms of their candidacy for alternate renewable fuels, Bioenergy Res., 6 (2013) 663–677.
[26] X. Wang, L. Xia, K. Tan, W. Zheng, Studies on adsorption of uranium(VI) from aqueous solution by wheat straw, Environ. Prog. Sustainable Energy, 31 (2012) 566–576.
[27] A. Garcia-Maraver, J. Perez-Jimenez, F. Serrano-Bernardo, M. Zamorano, Determination and comparison of combustion kinetics parameters of agricultural biomass from olive trees, Renewable Energy, 83 (2015) 897–904.
[28] D.-X. Ding, X.-T. Liu, N. Hu, G.-Y. Li, Y.-D Wang, Removal and recovery of uranium from aqueous solution by tea waste, J. Radioanal. Nucl. Chem., 293 (2012) 735–741.
[29] J. Yang, B. Volesky, Biosorption of uranium on *Sargassum* biomass, Water Res., 33 (1999) 3357–3363.
[30] Z. Aly, V. Luca, Uranium extraction from aqueous solution using dried and pyrolyzed tea and coffee wastes, J. Radioanal. Nucl. Chem., 295 (2013) 889–900.
[31] P.L.J. Kenney, E.M. Kirby, J. Cuadro, D.J. Weiss, A conceptual model to predict uranium removal from aqueous solutions in water–rock systems associated with low- and intermediate-level radioactive waste disposal, RSC Adv., 7 (2017) 7876–7884.
[32] A. Monji, V. Ghoulipour, M. Mallah, B. Maraghe-Mianji, Selective sorption of thorium(IV) from highly acidic aqueous

solutions by rice and wheat bran, J. Radioanal. Nucl. Chem., 303 (2015) 949–958.
[33] E. Bursali, M. Merdivan, M. Yurdakoc, Preconcentration of uranium(VI) and thorium(IV) from aqueous solutions using low-cost abundantly available sorbent, J. Radioanal. Nucl. Chem., 283 (2010) 471–476.
[34] P.D. Bhalara, D. Punetha, K. Balasubramanian, Kinetic and isotherm analysis for selective thorium(IV) retrieval from aqueous environment using eco-friendly cellulose composite, Int. J. Environ. Sci. Technol., 12 (2015) 3095–3106.
[35] M. Torab-Mostaedi, M. Asadollahzadeh, A. Hemmati, A. Khosravi, Biosorption of lanthanum and cerium from aqueous solutions by grapefruit peel: equilibrium, kinetic and thermodynamic studies, Res. Chem. Intermed., 41 (2013) 559–573.
[36] H. Parab, S. Joshi, N. Shenoy, R. Verma, A. Lali, M. Sudersanan, Uranium removal from aqueous solution by coir pith: equilibrium and kinetic studies, Bioresour. Technol., 96 (2005) 1241–1248.
[37] M. Lahiji, A. Keshtkar, M. Moosavian, Adsorption of cerium and lanthanum from aqueous solutions by chitosan/polyvinyl alcohol/3 mercaptopropyltrimethoxysilane beads in batch and fixed-bed systems, Part. Sci. Technol., 36 (2016) 340–350.
[38] K. Foo, B. Hameed, Insights into the modeling of adsorption isotherm systems, Chem. Eng. J., 156 (2010) 2–10.
[39] A. Monji, V. Ghoulipour, M. Mallah, Biosorption of toxic transition metals and radionuclides from aqueous solutions by agro-industrial by-products, J. Hazard. Toxic Radioact. Waste, 20 (2016), doi: 10.1061/(ASCE)HZ.2153-5515.0000296.
[40] M. Mahmoud, Removal of uranium(VI) from aqueous solution using low cost and ecofriendly adsorbents, J. Chem. Eng. Process. Technol., 4 (2013) 1–4.
[41] M. Al-Masri, Y. Amin, B. Al-Akel, T. Al-Naama, Biosorption of cadmium, lead, and uranium by powder of poplar leaves and branches, Appl. Biochem. Biotechnol., 160 (2010) 976–987.
[42] S. Zafar, N. Khalid, M. Daud, M. Mirza, Kinetic studies of the adsorption of thorium ions onto rice husk from aqueous media: linear and nonlinear approach, The Nucleus, 52 (2015) 14–19.
[43] R. Donat, A. Akdogan, E. Erdem, H. Cetisli, Thermodynamics of Pb^{2+} and Ni^{2+} adsorption onto natural bentonite from aqueous solutions, J. Colloid Interface Sci., 286 (2005) 43–52.
[44] U. Alkaram, A. Mukhlis, A. Al-Dujaili, The removal of phenol from aqueous solutions by adsorption using surfactant-modified bentonite and kaolinite, J. Hazard. Mater., 169 (2009) 324–332.
[45] S. Bagherifam, A. Lakzian, S. Ahmadi, M. Rahimi, A. Halajnia, Uranium removal from aqueous solutions by wood powder and wheat straw, J. Radioanal. Nucl. Chem., 283 (2010) 289–296.